Interactions of Porphyrins with Nucleic Acids†

Robert F. Pasternack,* Esther J. Gibbs,*,‡ and Joseph J. Villafranca§

ABSTRACT: The interactions of tetrakis(4-*N*-methylpyridyl)-porphine (H_2TMpyP-4) and its copper(II), nickel(II), zinc(II), cobalt(III), iron(III), and manganese(III) derivatives with several nucleic acids have been investigated. Spectrophotometric titrations of H_2TMpyP-4 and Cu(II)TMpyP-4 with the synthetic polymer poly(dG-dC) could be analyzed by a nearest-neighbor exclusion model leading to $n \approx$ two base pairs and equilibrium constants of 7.7×10^5 M^{-1} and 8.0×10^5 M^{-1}, respectively. The other metal derivatives [except for the nickel(II) porphyrin] do not provide sufficiently large color changes with poly(dG-dC) to allow analysis. In contrast, all of these porphyrins interact with poly(dA-dT) and DNA. For those porphyrins investigated, the binding profiles are not adequately fit by a nearest-neighbor exclusion model but have profiles suggesting that cooperativity effects are important. Spectral and circular dichroic experiments both suggest base specificity. With calf thymus DNA, the copper(II) and nickel(II) derivatives show prominent negative circular dichroism (CD) features and large red shifts and hypochromicity of the Soret absorption band characteristic of GC specificity, as demonstrated with the synthetic polymer. The other metal derivatives show prominent positive induced visible CD features with small red shifts and hypochromicity of the absorption bands in the Soret region characteristic of AT specificity. Only the metal-free derivative has a conservative CD spectrum suggesting distribution among GC and AT sites.

Recent investigations of porphyrin–nucleic acid interactions have led to the unanticipated result that the meso-substituted porphyrin, tetrakis(4-*N*-methylpyridyl)porphine (H_2TMpyP-4, Figure 1) is capable of intercalating in calf thymus DNA (Fiel et al., 1979; Fiel & Munson, 1980). As for other intercalated complexes, it is observed that (i) the DNA helix is stabilized against thermal denaturation, (ii) the ultraviolet spectral bands of DNA (as well as the Soret band of the porphyrin) display hypochromicity, (iii) the porphyrin drug has an induced optical activity in the visible region, (iv) the ellipticity in the near ultraviolet for DNA is altered, (v) there is an increase in the relative viscosity of solutions of these complexes indicating a lengthening of the DNA chain, and (vi) binding of the porphyrin results in an unwinding of covalently closed superhelical DNA.

Whereas a substantial number of other drugs have been shown to intercalate in DNA, these drugs are characteristically readily accommodated by the nucleic acid. That is, they are usually small, planar, aromatic molecules that can slip between adjacent base pairs of double-stranded nucleic acids without requiring major distortions from the idealized B form. However, an X-ray structure determination of a metal derivative of the very similar tetraphenylporphine reveals that the phenyl meso substituents are nearly perpendicular to the plane of the porphyrin ring (Scheidt, 1974) and thus might be expected to provide severe steric hindrance for intercalation. With molecular models, a stable structure for the B-DNA–H_2TMpyP-4 complex can be constructed in which the porphyrin core is intercalated and the positively charged; meso substituents interact with the negatively charged phosphate groups of the DNA backbone (H. M. Sobell, personal communication). However, unlike other intercalating drugs, the DNA portion of the model must be constructed around the porphyrin, and once formed, the porphyrin moiety cannot slide out of the DNA. Hence, the mechanistic details of the porphyrin intercalation process promise to provide useful information concerning the structure and flexibility of DNA in solution.

Among the processes that must be considered is the rotation of the *N*-methylpyridyl groups to a position more nearly coplanar to the porphyrin core. The rotational barrier to coplanarity has been measured for the indium, titanium, and ruthenium tetraphenylporphines as $\Delta G^{\ddagger} \sim 15$ kcal/mol if the ortho position of the meso-substituent ring system is occupied by hydrogen and coplanarity of the meso substituents is required (Eaton & Eaton, 1975; Eaton et al., 1978). This rather substantial barrier would predict a significant slowing of the intercalation process relative to other drugs. However, if rotation of the rings is unimportant, then the interaction of H_2TMpyP-2 (cf. Figure 1) with nucleic acids would be expected to duplicate that of H_2TMpyP-4. The barrier to rotation of the meso substituents is considerably greater than ~15 kcal/mol when *N*-methyl groups are in the ortho position (Eaton et al., 1978). Should structures more open than B-form DNA exist in solution, the steric barrier due to the *meso*-pyridyl substituents would play less of a role in determining intercalation extent and rate. Nucleic acid structures of this type have been proposed, including a β-kinked form of DNA that involves highly flexible, open regions in the duplex where hydrogen bonds have broken and bases unstacked (Sobell et al., 1977; Sobell, 1980). Crothers and co-workers have interpreted results for the binding of irehdiamine to DNA as being consistent with such a β-kinked structure for the complex (Dattagupta et al., 1978).

An additional advantage of the porphyrin system as a probe of DNA structure in solution is the availability of a variety of metal derivatives. The nature of the interaction with DNA can therefore be further examined by, for example, considering metalloporphyrins without axial ligands [e.g., copper(II) and nickel(II)], one axial ligand [e.g., zinc(II) and iron(III)], or two axial ligands [e.g., manganese(III), iron(III), nickel(II), and cobalt(III)]. These axially liganded derivatives might well serve as "molecular calipers" for the limiting thickness of an intercalating drug.

† From the Department of Chemistry, Swarthmore College, Swarthmore, Pennsylvania 19081 (R.F.P.), and the Department of Chemistry, The Pennsylvania State University, University Park, Pennsylvania 16802 (E.J.G. and J.J.V.). *Received November 17, 1982.* This research has been supported by grants from the National Institutes of Health (GM-17574) to R.F.P. and the National Science Foundation (PCM-8108094) to J.J.V.

‡ Present address: Department of Chemistry, Goucher College, Towson, MD 21204.

§ J.J.V. is an Established Investigator of the American Heart Association.

0006-2960/83/0422-2406$01.50/0

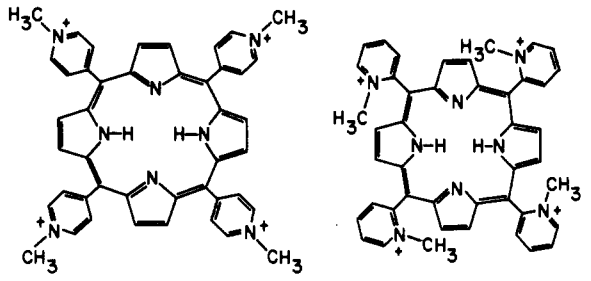

FIGURE 1: Structures of metal-free porphyrins used in the present study: (left) tetrakis(4-*N*-methylpyridyl)porphine (H_2TMpyP-4); (right) tetrakis(2-*N*-methylpyridyl)porphine (H_2TMpyP-2).

The present paper deals with the static experiments that have been conducted with porphyrin–nucleic systems. The kinetics of porphyrin–nucleic acid interactions have also been studied by us and will be reported in a later paper.

Materials and Methods

Calf thymus DNA was purchased from Worthington Biochemical Co. or Sigma Chemical Co. Samples of 1–2 mg of DNA/mL were dissolved by slowly stirring solutions overnight at 4 °C in phosphate buffer ([Na^+] = 0.2 M; pH 6.8). Protein was removed from the DNA by repeated extraction with a chloroform–isoamyl alcohol mixture at a ratio of 24:1. After the final centrifugation, the top two-thirds of the solution was carefully pipetted off and exhaustively dialyzed against buffer at the appropriate ionic strength. Poly(dG-dC) and poly(dA-dT) were purchased from P-L Biochemicals, Inc. Stock solutions of these two synthetic polymers were prepared by dissolving the materials in 0.019 M phosphate buffer at room temperature and at an ionic strength of 0.2 M. Solutions of approximately 1.5×10^{-3} M were frozen until use. The integrity of the nucleic acid duplexes was determined by comparing their UV and circular dichroism (CD) spectra with published results (Wells et al., 1970). Concentrations, always calculated in base pairs, were determined spectrophotometrically with $\epsilon^{262nm} = 1.32 \times 10^4$ M^{-1} cm^{-1} for poly(dA-dT) (Schmechel & Crothers, 1971), $\epsilon^{254nm} = 1.68 \times 10^4$ M^{-1} cm^{-1} for poly(dG-dC) (Müller & Crothers, 1968), and $\epsilon^{260nm} = 1.31 \times 10^4$ M^{-1} cm^{-1} for DNA (Wells et al., 1970).

The two nonmetalloporphyrins, H_2TMpyP-4 and H_2TMpyP-2, were purchased from Man-Win Coordination Chemicals as the tosylate salts and were used without further purification. The copper(II), cobalt(III), manganese(III), iron(III), nickel(II), and zinc(II) derivatives of H_2TMpyP-4 were prepared, purified, and converted to their chloride forms by a slightly modified published procedure (Pasternack et al., 1977, 1974): A 250-mg sample of H_2TMpyP-4 was dissolved in 100 mL of water, and the solution was stirred for 30 min and then filtered. The filtrate was transferred to the reaction vessel and brought to reflux. An approximately 500-fold excess (~0.1 mol) of the appropriate metal salt was added. The metal salts used in this study were $CoCl_2 \cdot 6H_2O$, $NiCl_2 \cdot 6H_2O$, $CuCl_2 \cdot 4H_2O$, $FeCl_2 \cdot 4H_2O$, and $MnCl_2 \cdot 2H_2O$. The solution was allowed to continue refluxing until no further changes of the visible spectrum were observed. The visible spectrum of the nonmetallo derivative is characterized by an intense Soret band at 423 nm and four weaker visible bands at longer wavelengths. A convenient monitor of metal insertion, especially for the copper(II) and iron(III) derivatives, which display no shifting of the nonmetallo Soret band, is the conversion of the four visible bands to a two visible band spectrum upon metal incorporation. The manganese(II), iron(II), and cobalt(II) ions are oxidized to the 3+ oxidation state upon insertion in the presence of oxygen. The nickel(II) and cobalt(III) derivatives were generally refluxed overnight whereas for the other metals only 1–2 h of refluxing was necessary. The solutions were then cooled in an ice bath, and excess sodium perchlorate was added to the reaction mixture to precipitate the metalloporphyrin product. The reaction mixture, which had a cloudy appearance at this point, was allowed to stand overnight, filtered, and washed 6–7 times with dilute (~2%) perchloric acid to remove excess metal ions. The resulting paste was transferred with 0.05 M hydrochloric acid to an ion-exchange column of Bio-Rad AG-1X8 in the chloride form to exchange away the perchlorate anion. The metalloporphyrin product was obtained by lyophilization. The spectral characteristics of the isolated materials were compared to literature values and found to be in excellent agreement. Concentrations were determined spectrophotometrically with $\epsilon^{424nm} = 2.26 \times 10^5$ M^{-1} cm^{-1} for H_2TMpyP-4 (Pasternack et al., 1972), $\epsilon^{424nm} = 2.31 \times 10^5$ M^{-1} cm^{-1} for Cu(II)TMpyP-4 (Pasternack et al., 1973), $\epsilon^{418nm} = 1.49 \times 10^5$ M^{-1} cm^{-1} for Ni(II)TMpyP-4 (Pasternack et al., 1974), $\epsilon^{434nm} = 2.15 \times 10^5$ M^{-1} cm^{-1} for Co(III)TMpyP-4 (Pasternack & Cobb, 1973), $\epsilon^{437nm} = 2.04 \times 10^5$ M^{-1} cm^{-1} for Zn(II)TMpyP-4 (Pasternack et al., 1973), $\epsilon^{403nm} = 1.02 \times 10^5$ M^{-1} cm^{-1} for Fe(III)-TMpyP-4 (Pasternack et al., 1977), $\epsilon^{463nm} = 0.92 \times 10^5$ M^{-1} cm^{-1} cm^{-1} for Mn(III)TMpyP-4 (Harriman & Porter, 1979), and $\epsilon^{414nm} = 1.82 \times 10^5$ M^{-1} cm^{-1} for H_2TMpyP-2 (Hambright et al., 1976).

All other chemicals were reagent grade and were used without further purification. All experiments, except where specifically indicated, were carried out at 25 °C, at pH 6.8, and in a phosphate buffer containing 0.006 M Na_2HPO_4, 0.02 M NaH_2PO_4, 0.001 M ethylenediaminetetraacetic acid (EDTA) (μ = 0.017), and sufficient NaCl to give a final ionic strength of μ = 0.2 M.

Spectral measurements were carried out on a Cary 14 double-beam recording spectrophotometer with a thermostated cell compartment. Absorbance titrations were conducted by adding concentrated stock solutions of the nucleic acids directly to a 10-mm curvette. Circular dichroism spectra were recorded on a Jasco J-40 spectropolarimeter at a spectral band-pass of 2 nm, made available by Dr. Douglas Turner at Rochester University. The wavelength was calibrated with a solution of *d*-10-camphorsulfonic acid.

Results

Absorption Spectra of Nucleic Acid–Porphyrin Complexes. The interaction of H_2TMpyP-2, H_2TMpyP-4, and several of the metal derivatives of the latter porphyrin were monitored with visible absorption spectroscopy. Table I presents a summary of the changes in the Soret band upon reaction of each of the porphyrins with DNA, poly(dA-dT), and poly(dG-dC) at $r_0 \leq 0.03$ (r_0 is defined as the ratio of the total concentration of porphyrin to that of nucleic acid in base pairs). For H_2TMpyP-4 as well as its copper(II) and nickel(II) derivatives, reaction with poly(dG-dC) leads to a substantial red shift of the Soret maximum and a large hypochromicity. Neither H_2TMpyP-4 nor Cu(II)TMpyP-4 adds axial ligands, while the metal ion in Ni(II)TMpyP-4 can be either four-coordinate with no axial ligands or six-coordinate with two axial ligands (Pasternack et al., 1973, 1974). In aqueous solution, Ni(II)TMpyP-4 displays a complicated spectrum in the Soret region consisting of two overlapping bands of comparable intensity, one at 417 nm due to the diamagnetic four-coordinate form and one at 442 nm due to the paramagnetic diaquo complex. It is suggested that the 434-nm Soret maximum for Ni(II)TMpyP-4 with poly(dG-dC) arises from a red shift of

Table I: Effect of Nucleic Acids on Wavelength Maximum of the Soret Band for Several Porphyrins and Metalloporphyrins for $0.020 \leq r_0 \leq 0.031$ [a]

porphyrin	λ_{max} (nm)	calf thymus DNA		poly(dG-dC)		poly(dA-dT)	
		λ_{max} (nm)	% H	λ_{max} (nm)	% H	λ_{max} (nm)	% H
H_2TMpyP-4	423	430	40	444	41	430	7
Cu(II)TMpyP-4	424	430	18	440	35	427	−2
Ni(II)TMpyP-4	417/442	434	38	434	46	423	20
Zn(II)TMpyP-4	437	439	−5	437	4	439	−6
Co(III)TMpyP-4	434	439	−27	434	6	439	−14
Fe(III)TMpyP-4	424	430	12	424	−2	429	9
Mn(III)TMpyP-4	463	463	−30	463	5	463	−26
H_2TMpyP-2	414	414	0	414	−3	415	−2

[a] The % hypochromicity (% H) was determined from $(\epsilon_p - \epsilon_b)/\epsilon_p \times 100$, where p represents free porphyrin, b represents bound porphyrin, and ϵ_p and ϵ_b were determined at the respective Soret maxima. A negative hypochromicity therefore demonstrates hyperchromicity. μ = 0.2 M; pH 6.8; 25 °C.

the 417-nm four-coordinate species; a blue shift of the Soret band has not been observed with any other porphyrin derivative upon binding to any of the nucleic acids. Thus the nickel(II) derivative is similar to the copper(II) derivative and nonmetalloporphyrins in that the basic structure for interaction with poly(dG-dC) is a four-coordinate, nonaxially liganded species. For the Zn(II)TMpyP-4, Co(III)TMpyP-4, Fe(III)TMpyP-4, and Mn(III)TMpyP-4 interactions with poly(dG-dC), there is no shift of the Soret maximum and virtually no hypochromicity; the iron(III) derivative even displays a small hyperchromicity. All four of these metalloporphyrins have axial ligands that would have to be accommodated between the base pairs of the nucleic acid and thus provide a steric barrier for intercalation. In summary, for poly(dG-dC), those metalloporphyrins that maintain axial ligands exhibit minor perturbations of their Soret maxima in contrast to those porphyrins without axial ligands for which the Soret maxima are substantially red shifted with large hypochromicity. These results suggest that the latter porphyrins interact to a larger content with the bases of poly(dG-dC) than do the metalloporphyrins that maintain their axial ligands. The presence of axial ligands may limit these latter porphyrins largely to an electrostatic type of bonding to the phosphate backbone and minimal interaction with the bases of the polynucleotide.

Changes in the Soret region of Cu(II)TMpyP-4, Ni(II)-TMpyP-4, and H_2TMpyP-4 upon interaction with poly(dA-dT) are not as large as those observed with poly(dG-dC). Cu(II)TMpyP-4 displays a very small red shift and hyperchromicity of the Soret maximum upon addition of poly(dA-dT). H_2TMpyP-4 has a relatively small hypochromicity with a slightly larger red shift than that of the copper(II) derivative. Ni(II)TMpyP-4 displays a shifting of the Soret maximum similar to that observed for Cu(II)TMpyP-4 and H_2TMpyP-4 with poly(dA-dT) but with a much larger hypochromicity than is observed with either of the other two species. Conversely, for the zinc(II), cobalt(III), iron(III), and manganese(III) derivatives, larger spectral changes are observed for reaction with poly(dA-dT) than with poly(dG-dC). Still, the perturbations of the Soret maxima for these latter porphyrins induced by poly(dA-dT) are in general substantially smaller than the perturbations caused by poly(dG-dC) on the Soret maxima of the copper(II), nickel(II), and metal-free porphyrins. This suggests that the axially liganded metalloporphyrins are able to interact more intimately with the bases of poly(dA-dT) than of poly(dG-dC) but that the interaction of these derivatives may not be as extensive as for the nonaxially liganded derivatives. The nickel(II) porphyrin is unique in that it is the only derivative that displays a large hypochromicity with poly(dA-dT). As will be discussed below, this metalloporphyrin also has a unique visible CD spectrum with poly(dA-dT).

The absorption results in the Soret region for H_2TMpyP-4 and Cu(II)TMpyP-4 with calf thymus DNA are intermediate between those obtained for the two synthetic nucleic acids. For these two porphyrins with calf thymus DNA, there appear to be interactions at both GC and AT sites. Ni(II)TMpyP-4, on the other hand, has a Soret maximum and hypochromicity similar to that obtained with poly(dG-dC), suggesting a higher degree of GC selectivity. For the class of axially liganded metalloporphyrins [i.e., zinc(II), iron(III), manganese(III), and cobalt(III) derivatives], changes in the Soret region with DNA are similar to those obtained upon binding to poly(dA-dT).

The H_2TMpyP-2 derivative was also considered via visible absorption spectroscopy. The Soret band for this porphyrin is virtually unaffected by the addition of any of the nucleic acids. The only change observed is a moderate hyperchromicity with poly(dA-dT) and poly(dG-dC). We conclude that H_2TMpyP-2, unlike H_2TMpyP-4, interacts only weakly with the bases of any of the nucleic acids. H_2TMpyP-2 has no axial ligands, but the location of the *N*-methyl group in the ortho position of the pyridine ring presents a large barrier to rotation of the meso substituent about its C_4–C_{meso} bond axis. This tends to lock the *N*-methylpyridyl ring in a position roughly perpendicular to the plane of the porphyrin core, and this additional steric bulk hinders the insertion of this porphyrin between the bases of the helix, preventing the formation of an intercalated complex.

Titrations of H_2TMpyP-4 and Cu(II)TMpyP-4 with DNA, poly(dA-dT), and poly(dG-dC) were conducted. As may be seen from Figure 2, the interaction of H_2TMpyP-4 with poly(dG-dC) produces an isosbestic point at 436 nm. The data were analyzed with the McGhee–von Hippel approach derived for the binding of drugs to homogeneous one-dimensional polynucleotide lattices, and which incorporates neighbor exclusion effects (McGhee & von Hippel, 1974). For noncooperative binding, the equation is of the form

$$r/m = K_{app}(1 - nr)\left[\frac{1 - nr}{1 - (n - 1)r}\right]^{n-1} \quad (1)$$

where r is defined as the number of moles of bound porphyrin per mole of total base pairs, m is the molar concentration of free porphyrin, n is the number of consecutive lattice residues made inaccessible by the binding of a single drug molecule, and K_{app} is the apparent affinity constant for the porphyrin binding to a site on the nucleic acid. Values of r and m necessary for the analysis were calculated by the method of Peacocke & Sherrett (1956). This method requires a value

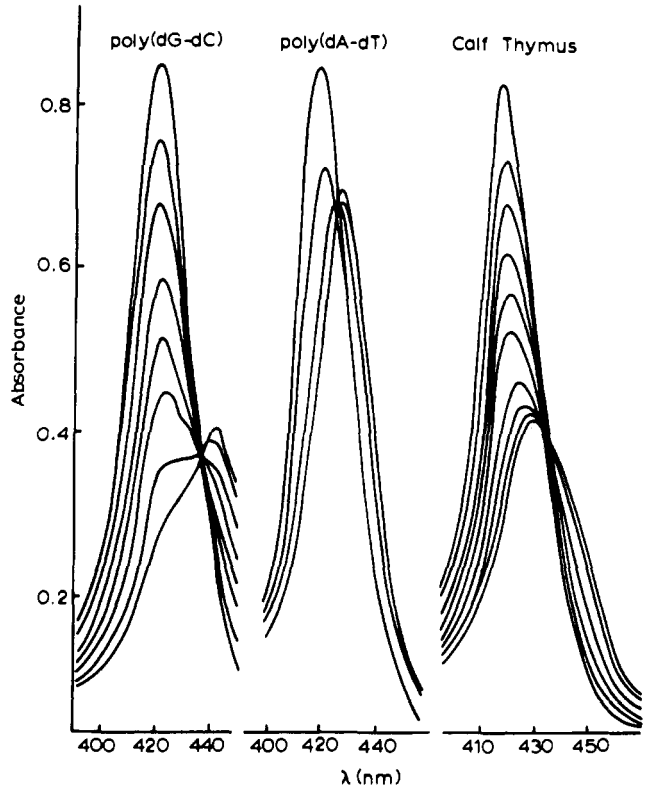

FIGURE 2: Titration of H_2TMPyP-4 with nucleic acids: μ = 0.2 M, pH 6.8, 25 °C.

	$[H_2TMpyP\text{-}4]$	range of $1/r_0$
poly(dG-dC)	3.6×10^{-6} M	0-4
poly(dA-dT)	3.6×10^{-6} M	0-10
DNA	3.6×10^{-6} M	0-7.6

for ϵ_b, the molar absorptivity of the bound porphyrin. A value of $\epsilon_b^{exptl} = 5.07 \times 10^4$ M^{-1} cm^{-1} at 423 nm was determined by measuring the absorption of a solution in which the base-pair concentration was 70 times greater than the H_2TMPyP-4 concentration, conditions for which complete binding may be assumed. It is observed in the titration that when the total base-pair concentration is greater than 15–20 times the porphyrin concentration, no further changes in the Soret band occur. Solutions with a 30–70-fold excess of poly(dG-dC) gave identical values for ϵ_b^{exptl}, indicating that within experimental error all of the porphyrin is bound at these ratios. A plot of the data at μ = 0.2 M according to eq 1 is nonlinear as shown in Figure 3. McGhee and von Hippel have shown that, in the special case of a homogeneous one-dimensional lattice, curvature can arise as a consequence of neighbor exclusion effects. The intercept on the r/m axis is K_{app}, and the intercept on the r axis is $1/n$. The determination of n from the intercept on the r axis by extrapolation of the data is subject to large uncertainties. However, as shown by McGhee and von Hippel, the value of n can be obtained more precisely from the derivative of eq 1 in the limit of low r:

$$\lim_{r \to 0} \frac{d(r/m)}{dr} = -K_{app}(2n - 1) \qquad (2)$$

This limiting slope line intercepts the abscissa at a value of $(2n - 1)^{-1}$ and has a slope of $-K_{app}(2n - 1)$. For H_2TMPyP-4 and Cu(II)TMPyP-4, values of $K_{app} = 7.7 \times 10^5$ M^{-1} and 8.0×10^5 M^{-1} and n = 1.8 and 1.8 were obtained, respectively. These values of n indicate that about two lattice sites are made unavailable for every ligand that binds. Using a similar approach, Fiel and co-workers obtained a value for the

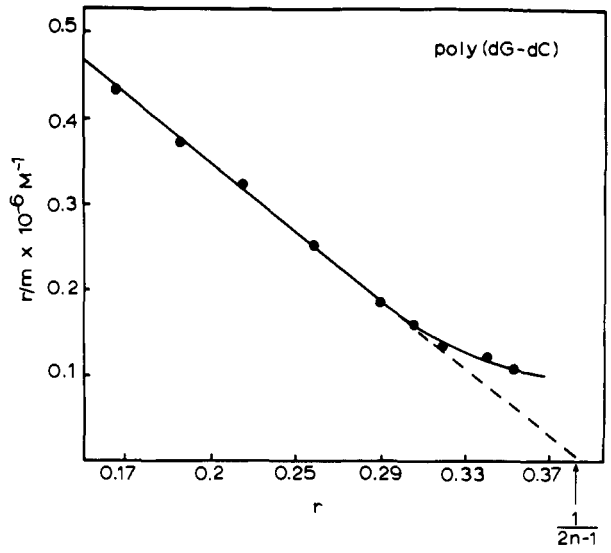

FIGURE 3: Binding isotherm for titration of H_2TMPyP-4 with poly(dG-dC): $[H_2TMPyP\text{-}4] = 2.6 \times 10^{-6}$ M; $0.39 < 1/r_0 < 6.4$; μ = 0.2 M; pH 6.8; 25 °C; $K_{app} = 7.7 \times 10^5$ M^{-1}; n = 1.8.

H_2TMPyP-4/poly(dG-dC) system of $K_{app} = 6.3 \times 10^4$ M^{-1} and $n \simeq 2.3$ at μ = 0.5 M (R. Fiel and M. Carvlin, personal communication).

Similar titrations at μ = 0.2 M were conducted for H_2TMPyP-4 with poly(dA-dT); the absorbance changes upon addition of Cu(II)TMPyP-4 to poly(dA-dT) are too small for analysis. The Soret band shows a red shift from 423 to 430 nm and relatively small hypochromicity when compared to those of the poly(dG-dC) complex (Figure 2). Unlike poly(dG-dC), there is no isosbestic point, and near the end of the poly(dA-dT) titration the absorbance no longer continues to decrease but displays a small *absorbance increase*. The apparent molar absorptivitiy (ϵ_{app} = absorbance/$[H_2TMPyP\text{-}4]_{total}$) reaches a minimal value in the titration at 423 nm of 1.37×10^5 M^{-1} cm^{-1} and then increases. When the molar absorptivity of the complex was determined by measuring the absorption of a solution with a 60-fold excess of poly(dA-dT) over porphyrin, a ratio at which binding should be complete, a value of $\epsilon_b^{exptl} = 1.45 \times 10^5$ M^{-1} cm^{-1} at 423 nm was obtained. These results indicate that the binding of H_2TMPyP-4 to poly(dA-dT) is more complicated than the binding to poly(dG-dC). In order to construct binding curves, a value for ϵ_b is required, but this parameter appears to vary as a function of r, a complication that renders data analysis difficult. McGhee–von Hippel type plots were constructed with various values for the molar absorptivity of the bound porphyrin. As shown in Figure 4, when values of $\epsilon_b < 1.35 \times 10^5$ M^{-1} cm^{-1} are used, the binding curves show curvature characteristic of positive cooperativity (McGhee & von Hippel, 1974). For large values of ϵ_b, including the independently determined value and the minimum ϵ_{app} of the titration, the general shape of the binding curve remains the same, but in the limit of low r, values for r/m become negative. It is clear that this synthetic homopolymer is manifesting behavior more complicated than can be explained by neighboring exclusion alone. Other effects such as (i) stacking (i.e., positive cooperativity), where the drugs interact directly on the poly(dA-dT) lattice, (ii) allosterism, where the drug molecules interact indirectly by altering the state of the polymer, and/or (iii) the existence of different structural complexes may be operating. Crothers and co-workers have reported examples of some of these phenomena (Dattagupta et al., 1980; Bresloff & Crothers, 1981). The dependence of ϵ_b binding on ratio makes

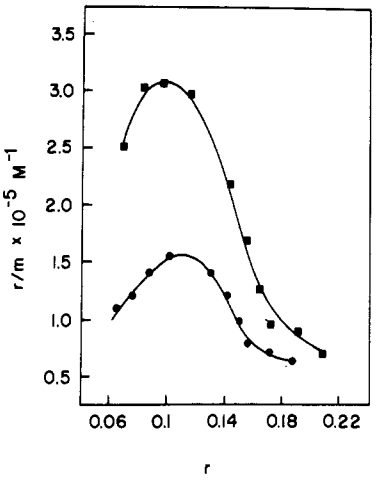

FIGURE 4: Binding isotherm for titration of H_2TMpyP-4 with poly(dA-dT) at various values of ϵ_b: [H_2TMpyP-4] = 3.6×10^{-6} M; $0.95 < 1/r_0 < 13.2$; μ = 0.2 M; pH 6.8; 25 °C; (■) $\epsilon_b = 1.3 \times 10^5$ M^{-1} cm^{-1}; (●) $\epsilon_b = 1.2 \times 10^5$ M^{-1} cm^{-1}.

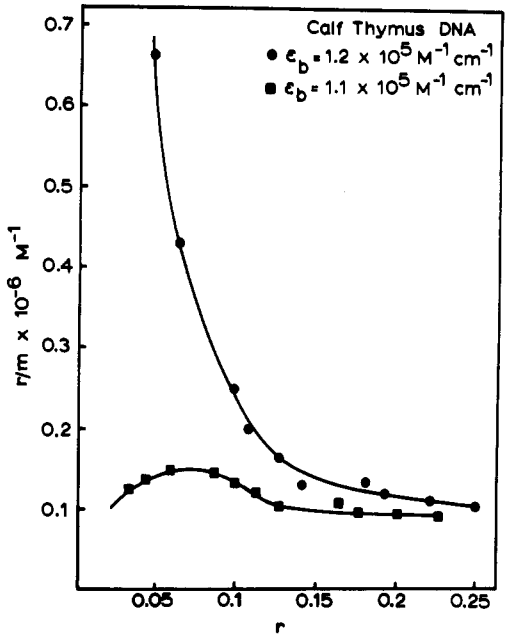

FIGURE 5: Binding isotherm for titration of H_2TMpyP-4 with calf thymus DNA at various ϵ_b: [H_2TMpyP-4] = 3.3×10^{-6} M; $0.75 < 1/r_0 < 13.1$; μ = 0.2 M; pH 6.8; 25 °C.

it difficult to extract quantitative information and to assess the relative importance of these phenomena. However, from the concentration range required for the titration, the value of K_{app} can be estimated to be within a factor of 10 of the value obtained for poly(dG-dC).

The binding characteristics of H_2TMpyP-4 with calf thymus DNA are intermediate between those of the two synthetic nucleic acids having features of both (Figure 2). A red shift from 423 to 430 nm is observed similar to that with poly(dA-dT) (albeit with a broad, long-wavelength shoulder), and there is a marked hypochromicity similar to that obtained for poly(dG-dC). The molar absorptivity of the porphyrin–DNA complex was determined experimentally as $\epsilon_b^{exptl} = 1.10 \times 10^5$ M^{-1} cm^{-1} by measuring the absorbance of a solution containing a 100-fold excess of DNA over H_2TMpyP-4 and assuming complete binding. McGhee–von Hippel type plots using this value for ϵ_b and ϵ_b^{exptl} + 10% are shown in Figure 5. For ϵ_b^{exptl} − 10%, the analysis yields negative values for r/m at low r values. Clearly, these profiles are very sensitive to the value

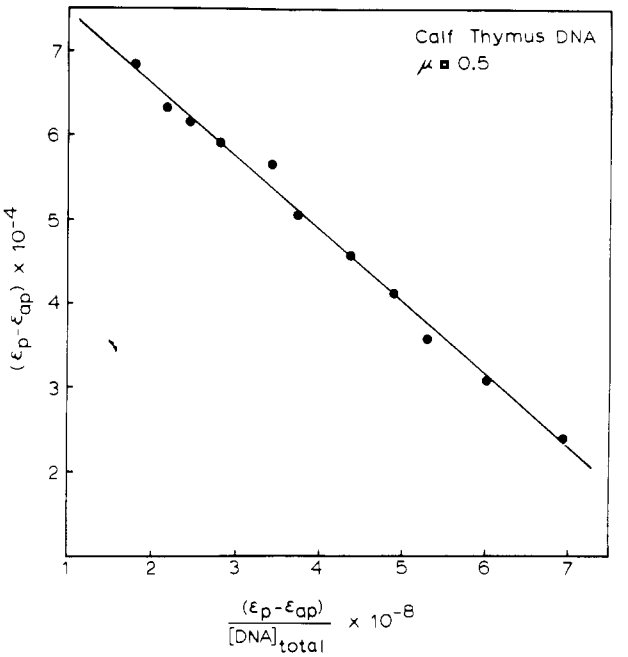

FIGURE 6: Binding isotherm for titration of H_2TMpyP-4 with calf thymus DNA according to eq 3 of text: 3.20×10^{-6} M ≤ [H_2TMpyP-4] ≤ 2.68×10^{-6} M; $10.8 \leq 1/r_0 \leq 144$; μ = 0.5 M; pH 6.8; 25 °C.

chosen for ϵ_b in that values agreeing to within experimental error lead to titration profiles suggestive of different binding models. The binding of H_2TMpyP-4 to DNA thus displays complexities similar to those observed for poly(dA-dT) and probably involves binding types seen with both poly(dG-dC) and poly(dA-dT). Since this nonmetallo derivative binds to both synthetic polynucleotides, it is not unreasonable to expect that it would bind to both types of sites on DNA, albeit with some degree of selectivity.

We have been able to obtain an estimate of K_{app} for the H_2TMpyP/DNA system by conducting titrations at ionic strengths greater than μ = 0.2. This experimental strategy takes advantage of the fact that the binding constant decreases with increasing ionic strength, and thus, throughout virtually all of the titration, the DNA concentration is in greater than 10-fold excess over the porphyrin concentration. Therefore, it can be assumed that the free DNA concentration is approximately equal to the total DNA concentration. Since r/m is equal to [complex]/([H_2TMpyP-4][DNA]$_{total}$), if [DNA]$_{total}$ ≃ [DNA]$_{free}$, then r/m is equal to K_{app} and is constant throughout the entire titration. This analysis also makes the further reasonable assumption that the value of n for neighbor exclusion is relatively small since values of 2–3 are most common. Using these assumptions, it can be shown that

$$\epsilon_p - \epsilon_{app} = \frac{\epsilon_{app} - \epsilon_p}{[DNA]_{total}} \frac{1}{K_{app}} + \Delta\epsilon \qquad (3)$$

where ϵ_p is the molar absorptivity of the free porphyrin, ϵ_{app} is the absorbance of a given solution divided by the total porphyrin concentration, and $\Delta\epsilon$ is $\epsilon_p - \epsilon_b$. Thus, a plot of $\epsilon_p - \epsilon_{app}$ vs. $(\epsilon_{app} - \epsilon_p)/[DNA]_{total}$ should yield a straight line of slope $1/K_{app}$ and an intercept of $\Delta\epsilon$. As shown in Figure 6, a plot of the data is linear, leading to a value for K_{app} of 1.2×10^4 M^{-1} and $\Delta\epsilon$ of 8.10×10^4 M^{-1} cm^{-1}, thereby giving $\epsilon_b = 1.24 \times 10^5$ M^{-1} cm^{-1} at 423 nm. This value for ϵ_b is in excellent agreement with the experimentally determined value of $\epsilon_b^{exptl} = 1.25 \times 10^5$ M^{-1} cm^{-1} obtained from the absorbance of a solution containing a 600-fold excess of DNA over por-

Table II: Percent of Free Porphyrin Soret Maximum Regained after Addition of 2 M NaCl to Solutions of Porphyrin and Nucleic Acid at 0.2 M NaCl for $r_0 \leq 0.03$, pH 6.8

porphyrin	percent free porphyrin absorbance regained		
	poly-(dG-dC)	poly-(dA-dT)	DNA
H_2TMpyP-4	98	98	98
Ni(II)TMpyP-4	44	10	30
Cu(II)TMpyP-4	73	66	67
Fe(III)TMpyP-4	96	92	91
Mn(III)TMpyP-4	100		100

phyrin. The value for K_{app} should be corrected for nearest-neighbor exclusion effects. Multiplication by 1.8, the factor determined at $\mu = 0.2$ M for poly(dG-dC), gives a K_{app}^{corr} value of $\sim 2 \times 10^4$ M^{-1}, similar to the value obtained for the H_2TMpyP/poly(dG-dC) system under similar conditions (R. Fiel and M. Carvlin, personal communication).

Spectral experiments were conducted in which porphyrin solutions preincubated with nucleic acid were diluted with sodium chloride solutions to yield a final ionic strength of 2.0 M. The results of these experiments are summarized in Table II. As was pointed out earlier for the H_2TMpyP-4 systems with poly(dG-dC) and DNA, the equilibrium constant for binding is ionic strength dependent. Thus, increases in salt concentration lead to dissociation of the porphyrin–nucleic acid complexes. It is observed that 2 M ionic strength almost completely dissociates the nonmetalloporphyrin complex from DNA, poly(dA-dT), and poly(dG-dC). Except for the nickel(II) and copper(II) derivatives, 2 M sodium chloride is sufficient to dissociate greater than 90% of all the complexes studied. The nickel(II) porphyrin complexes appear to be the most resistant to dissociation by high ionic strength. In particular, the nickel(II) porphyrin complex with poly(dA-dT) is only 10% dissociated at $\mu = 2$ M. From the titration data at $\mu = 0.2$ M, the nonmetallo and copper(II) derivatives appear to have about the same binding constants with poly(dG-dC). The extra stability of the copper(II) derivative at high ionic strength could be due to interactions of the metal centers with the bases of the nucleic acids via its vacant axial sites. This could also be true for the nickel(II) porphyrin, which has a greater tendency to add axial ligands than does the copper(II) derivative.

Circular Dichroism of Nucleic Acid–Porphyrin Complexes. The porphyrin and metalloporphyrin derivatives considered here do not display circular dichroism (CD) spectra in the absence of nucleic acids, but such spectra are induced for the various porphyrins with DNA and the two synthetic polynucleotides in the visible region. These effects are summarized

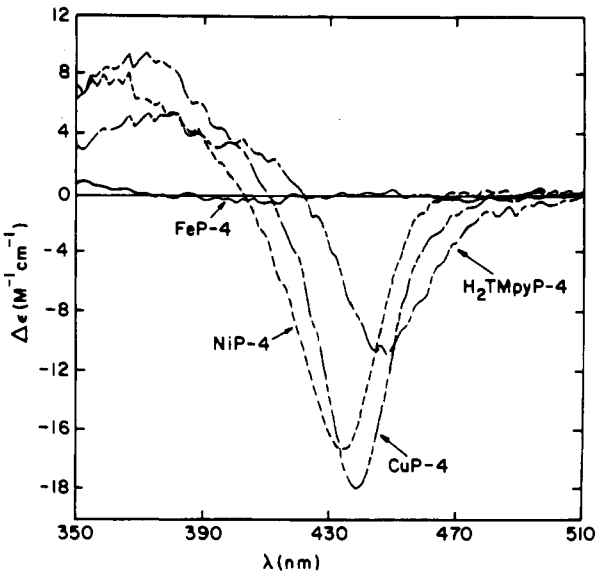

FIGURE 7: Induced circular dichroism spectra of porphyrins and metalloporphyrins with poly(dG-dC): $r_0 \simeq 0.03$; $\mu = 0.2$ M; pH 6.8; 25 °C.

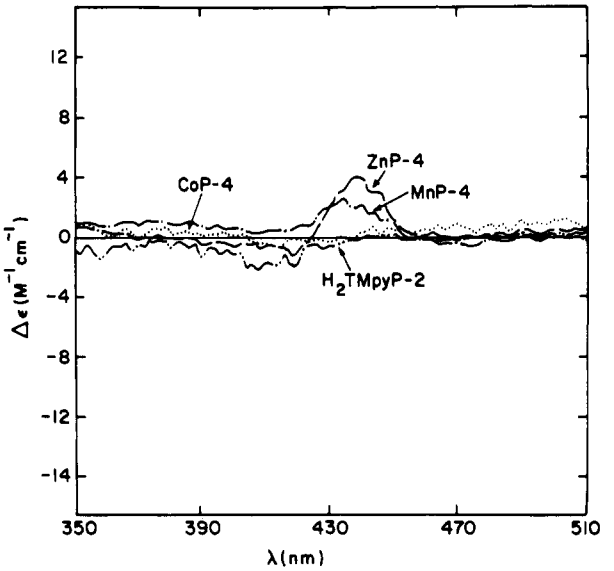

FIGURE 8: Induced circular dichroism spectra of porphyrins and metalloporphyrins with poly(dG-dC): $r_0 \simeq 0.03$; $\mu = 0.2$ M; pH 6.8; 25 °C.

Table III: Summary of Circular Dichroism and Absorbance Results in the Visible Region[a]

porphyrin	λ_{max}^{Soret} (nm)	calf thymus DNA		poly(dG-dC)		poly(dA-dT)	
		λ_{max}^{Soret} (nm)	CD	λ_{max}^{Soret} (nm)	CD	λ_{max}^{Soret} (nm)	CD
H_2TMpyP-4	423	430 (small, red shoulder)	+426 −448	444	−448	430	+433
Cu(II)TMpyP-4	424	430	−432 +415 (very small)	440	−439	427	+419 +438
Ni(II)TMpyP-4	417/442	434	−437	434	−434	423	+420 −439
Fe(III)TMpyP-4	424	430	+433	424	no band	429	+440
Co(III)TMpyP-4	434	439	+442	434	+440 (very small)	439	+434
Mn(III)TMpyP-4	463	463		463	no band	463	+464
Zn(II)TMpyP-4	437	439	+433, +455	437	+440, +450 (very small)	439	+424, +438
H_2TMpyP-2	414	414		414	no band	414	+420

[a] $\mu = 0.2$ M; pH 6.8; $r_0 \approx 0.03$; 25 °C.

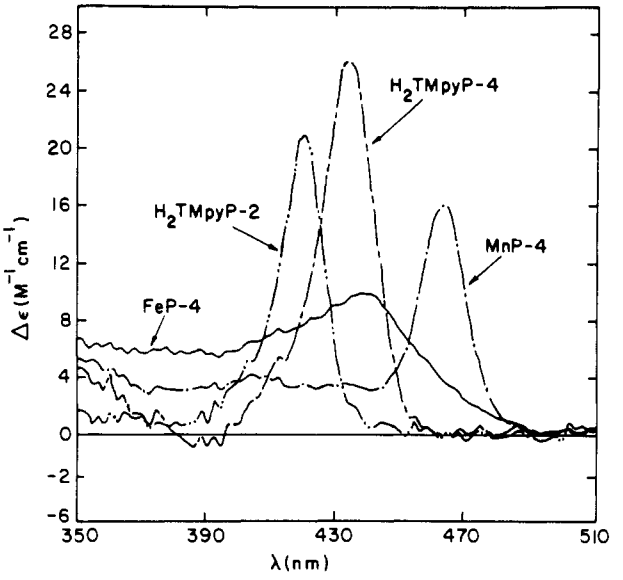

FIGURE 9: Induced circular dichroism spectra of porphyrins and metalloporphyrins with poly(dA-dT): $r_0 \simeq 0.03$; $\mu = 0.2$ M; pH 6.8; 25 °C.

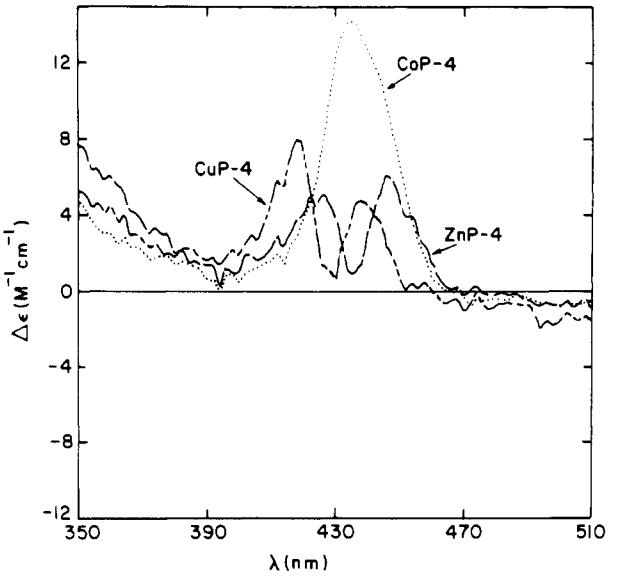

FIGURE 10: Induced circular dichroism spectra of metalloporphyrins with poly(dA-dT): $r_0 \simeq 0.03$; $\mu = 0.2$ M; pH 6.8; 25 °C.

in Table III and a number of representative spectra are shown in Figures 7–11. The nucleic acids have no absorption bands in the visible region, and therefore, only the induced CD of the porphyrins are observed. All of these spectra were obtained at excess nucleic acid, that is $r_0 < 0.03$.

With poly(dG-dC), copper(II), nickel(II), and metal-free H_2TMpyP-4 all display negative CD spectra with relatively large ellipticities. H_2TMpyP-2 and those metalloporphyrins that maintain axial ligands display either no CD spectrum at all or small positive bands. As also indicated by the visible absorption spectra, the CD results suggest that the interaction of this class of porphyrins with poly(dG-dC) is substantially limited by the presence of axial ligands or by substituents that freeze the *N*-methylpyridyl rings in a position perpendicular to the porphyrin core. Conversely, all of the porphyrins examined display large positive CD spectra with poly(dA-dT), except for the nickel(II) derivative, which has a conservative spectrum. Apparently, the poly(dA-dT) helix can accommodate the sterically hindered porphyrins more readily than can the poly(dG-dC) helix. Although the complexes formed

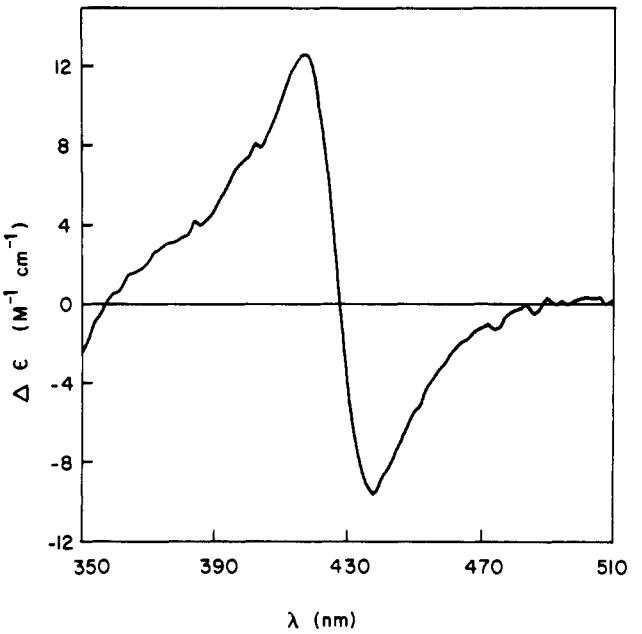

FIGURE 11: Induced circular dichroism spectra of Ni(II)TMpyP-4 with poly(dA-dT): $r_0 = 0.029$; $\mu = 0.2$ M; pH 6.8; 25 °C.

with poly(dA-dT) with the axially liganded metalloporphyrins or H_2TMpyP-2 may not be due to intercalation, they must involve more than purely electrostatic forces with the phosphate backbone. If only Coulombic forces were involved, then similar complexes would be expected with poly(dG-dC). These latter porphyrins may form complexes with poly(dA-dT) in which they are only partially intercalated or in which they are bound in a groove of the helix. It is known that poly(dA-dT) is far more flexible than poly(dG-dC) (Early et al., 1981a,b).

The induced CD spectra of Cu(II)TMpyP-4 and H_2TMpyP-4 with calf thymus DNA are composed of both positive and negative components (cf. Table III). For the copper(II) derivative, the positive band displays a much smaller ellipticity than the negative band. These spectra are similar to the visible CD spectrum observed for the proflavin with DNA (Dalgleish et al., 1969). Proflavin is a known intercalator, which has been shown to interact with both GC and AT sites. In contrast, the zinc(II), cobalt(III), and iron(III) derivatives of H_2TMpyP-4 display only a positive CD band in the visible range. This profile is similar to that of di-*tert*-butylproflavin (Dalgleish et al., 1972), whose bulky *tert*-butyl groups prevent intercalation and which shows a marked specificity for AT-rich DNA (Müller et al., 1973). These parallels with other systems, together with the negative CD observed for poly(dG-dC) complexes and the positive CD for poly(dA-dT) complexes, suggest that, for this case of porphyrins, at small values of r_0 a positive CD band is indicative of interactions with AT sites and a negative CD band with GC sites [with the notable exception of the nickel(II) derivative and poly(dA-dT) discussed below].

At this value of r_0 the nickel(II) derivative exhibits only a negative CD band with DNA. This suggests that in the presence of excess DNA, Ni(II)TMpyP-4 prefers to populate G-C base-pair sites. This conclusion correlates with the visible-absorption results in which the Soret region for the nickel porphyrin complex with DNA closely resembles the spectrum of the nickel(II) porphyrin complex with poly(dG-dC). The H_2TMpyP-4 complex with DNA has both positive and negative components; likewise, its absorption spectrum in the Soret region has features intermediate between the spectra observed for its complexes with poly(dA-dT) and poly(dG-dC), sug-

gesting that this nonmetallo derivative interacts significantly with both G-C and A-T pair sites.

The conservative CD spectrum of the nickel porphyrin with poly(dA-dT) is unique for this series of porphyrins at this value of r_0. This type of spectrum may result from the existence of two types of complexes or from the formation of a stacked outside-bound complex in which the nickel(II) porphyrin binds at lattice sites that are close to one another, resulting in an exciton-split spectrum (Tinoco & Cantor, 1970). As stated earlier, the nickel(II) porphyrin appears to bind to poly(dA-dT) as its four-coordinate species with its axial sites vacant. The additional chemistry that can occur at these vacant sites may well be responsible for either the existence of a second distinct complex with poly(dA-dT), whose negative sign might suggest it is more similar in structure to complexes formed with poly(dG-dC), or stacked aggregates along isolated regions of the poly(dA-dT) duplex.

Discussion

The spectral and circular dichroism evidence of the present study leads to the conclusion that, for the series of synthetic meso-substituted porphyrins investigated, the type of complex formed with GC-rich regions is fundamentally different from that formed in AT-rich regions. It is suggested on the basis of the combined evidence that the formation of a truly intercalated species requires G-C base pairs and that either a partially intercalated complex or an outside-bound complex (perhaps in a groove) is formed within the AT regions of DNA. The intercalated complex is characterized experimentally by (i) large red shifts of the Soret maximum ($\geq$15 nm), (ii) substantial hypochromicity of the Soret band ($\geq$35%), and (iii) a negative induced CD band in the Soret region. In addition, these intercalated porphyrin complexes show similar kinetic patterns. The details of these kinetic results will be reported in a later paper, but the generalizations that emerge include the following: (iv) the rates of formation and dissociation of these complexes have half-lives greater than 3 ms and (v) these complexes show observable temperature-jump relaxation effects (R. F. Pasternack et al., unpublished results).

Porphyrin complexes formed with AT regions are characterized by (i) small red shifts of the Soret maximum ($\leq$8 nm), (ii) small hypochromicity ($\leq$10%) or hyperchromicity of the Soret band, (iii) positive induced CD bands in the Soret region, (iv) rates for formation and dissociation of the complex that have half-lives less than 3 ms, and (v) no observable temperature-jump relaxation effects.

An important consideration in the use of the sign of the induced visible CD band as a marker for binding site specificity is the r_0 range in which this assignment is valid. All of the CD work in the present study was conducted at $r_0 \leq 0.03$. Since, except for the Fe(III)TMpyP-4, these porphyrins do not aggregate, it is not unreasonable to anticipate that at this large excess of base pairs to porphyrins stacking interactions will be minimal. At larger values of r_0 different types of bound complexes may begin to form, and especially for AT regions in which binding is on the outside of the helix, stacking may occur leading to exciton-split CD spectra. This exciton splitting can result in a conservative spectrum in which both positive and negative bands are present. Thus the use of the CD spectra to determine base-pair specificity may not be valid at larger values of r_0, when the nucleic acid is saturated with bound porphyrin molecules. For example, *meso*-tetrakis(*p*-trimethylaniliniumyl)porphine (H_2TAP) does not intercalate into DNA; presumably the bulky trimethylanilinium group prevents the passage through the DNA interior (Carvlin et al., 1982). For $r_0 \leq 0.045$, only positive bands are obtained in the Soret region of the CD spectrum similar to those of metalloderivatives of H_2TMpyP-4 having axial ligands and to di-*tert*-butylproflavin (Carvlin et al., 1982). However, at larger r_0 values ($r_0 \geq 0.128$) both positive and negative bands are obtained. It is perhaps worth noting that H_2TAP aggregates in aqueous solution at conditions for which H_2TMpyP is monomeric (W. P. Hambright, personal communication). This greater tendency toward aggregation for H_2TAP could well lead to more extensive porphyrin–porphyrin interaction in outside-bound forms.

The porphyrins and metalloporphyrins chosen for investigation present different types of steric barriers for intercalation into nucleic acids. The 4-*N*-methylpyridyl groups at the meso positions of H_2TMpyP-4 are nearly perpendicular to the plane of the porphyrin core (Scheidt, 1974), and NMR studies indicate the barrier to rotation of the groups is about 15 kcal/mol when hydrogen are in the ortho positions (Eaton & Eaton, 1975; Eaton et al., 1978). In order to facilitate intercalation, it is necessary for these rings to rotate toward a coplanar position, and/or intercalation occurs with a substantial disruption of the helical structure, leading to base-pair unstacking and/or opening, thereby allowing passage of the *N*-methylpyridyl groups through the helical structure. The H_2TMpyP-2 derivative was employed to elucidate the relative importance of these two effects. For this latter porphyrin, the placement of *N*-methyl groups in the ortho position greatly hinders rotation of the meso substituents (Eaton et al., 1978). For solutions of this porphyrin with poly(dG-dC), poly(dA-dT), and DNA, there is virtually no change in the Soret maximum, indicating minimal interaction with the bases of these duplexes. A substantial positive CD band is induced in the visible region with poly(dA-dT), but no band is observed with poly(dG-dC). Conversely, the interaction of H_2TMpyP-4 with poly(dG-dC) leads to a large red shift and hypochromicity of the Soret maximum and a negative induced CD band in the visible region. With poly(dA-dT), this latter porphyrin displays a larger red shifting and hypochromicity of the Soret band than observed for H_2TMpyP-2. Similar to the H_2TMpyP-2 porphyrin, the H_2TMpyP-4 porphyrin has a large positive CD band with poly(dA-dT). H_2TMpyP-2 does not intercalate into either poly(dG-dC) or poly(dA-dT) but binds to the outside of the helices. This is substantiated by the finding that H_2TMpyP-4 but not H_2TMpyP-2 unwinds covalently closed superhelical DNA, a property common to intercalating drugs (R. Fiel and M. Carvlin, personal communication; Delays & Jackson, 1976). Thus, the inability of the meso substituents to rotate toward a coplanar position prevents intercalation and severely limits the interaction of the porphyrin moiety with the bases of the nucleic acid. It should be noted that the complex between poly(dA-dT) and H_2TMpy-2 must involve more than Coulombic attractions or it would be anticipated that similar complexes could form with poly(dG-dC), and therefore, an induced CD would be observed in the visible region.

The influence of axial ligands on metalloporphyrin–nucleic acid interactions was also considered. Cu(II)TMpyP-4, which has no axial ligands, is very similar to nonmetallo H_2TMpyP-4 in its interactions with the two synthetic homopolymers. The Soret maximum of this metalloporphyrin is substantially red shifted upon binding to poly(dG-dC) with large hypochromicity, and a negative CD band is observed in the visible region. With poly(dA-dT), the copper(II) porphyrin does not display large changes in its Soret maximum, and positive CD bands appear in the visible region. As for H_2TMpyP-4, the negative CD band and large change of the Soret maximum

indicate that the copper(II) derivative intercalates into poly(dG-dC), whereas the relatively smaller changes of the Soret maximum and the positive CD bands in the visible region with poly(dA-dT) indicate an externally bound complex or perhaps partially intercalated species.

For those metalloporphyrins that maintain their axial ligands [the iron(III), cobalt(III), zinc(II), and manganese(III) derivatives of H_2TMpyP-4], no shifting of the Soret maxima and very small positive or no CD-induced bands are observed in the visible region with poly(dG-dC). With poly(dA-dT), these same metalloporphyrins have Soret maxima that are red shifted from 0 to 5 nm and have large, positive induced CD bands in the visible region. In addition, the cobalt(III) and manganese(III) derivatives both display substantial hyperchromicity with poly(dA-dT) rather than the usually observed hypochromism associated with intercalating molecules. By way of analogy, when proflavin intercalates into DNA, significant hypochromicity of its visible absorption band occurs, unlike the nonintercalating derivative, 2,7-di-*tert*-butylproflavin, which displays significant hyperchromicity (Müller et al., 1973). The additional steric constraints presented by the axial ligands at the metal center of the porphyrin serve to prevent intercalation into the nucleic acids. The diaxially liganded metalloporphyrins have a ligand–metal–ligand distance of approximately 7–10 Å, and the zinc(II) derivative, with its one axial ligand, has an approximately 5-Å thickness (Hoard, 1975). Thus, these helical structures cannot accommodate molecules, in an intercalated fashion, whose thicknesses approach 5 Å. An ambiguity that must be considered in using these axially liganded porphyrins as molecular calipers for intercalation is that the axial ligands may also be disrupting the stabilizing van der Waals π–π interactions between the porphyrin and the nucleic acid bases.

As with the H_2TMpyP-2 derivative, the interaction of these axially liganded metalloporphyrins is more severely limited with poly(dG-dC) than with poly(dA-dT). It is suggested that upon formation of these porphyrin–poly(dA-dT) complexes, some deformation of the helical structure occurs. The greater rigidity of the poly(dG-dC) helix relative to poly(dA-dT) (Early et al., 1981a,b) prevents such deformations and limits the interaction of the bulkier porphyrins to purely Coulombic attractions. It could be that these bulkier metalloporphyrins can be accommodated into a groove of the poly(dA-dT) helix but not into a poly(dG-dC) groove. This type of specificity for an outside-binding drug has also been observed for the nonintercalating proflavin derivative 2,7-di-*tert*-butylproflavin, which binds to DNA with a marked preference for AT regions (Müller et al., 1973).

In summary, we believe that complexes of several different types exist between nucleic acids and H_2TMpyP-4 and its metal derivatives. Furthermore, by judicious choice of metal derivatives, drugs showing high degrees of base specificity are obtained. Further evidence for these conclusions is obtained from kinetic results soon to be published (R. F. Pasternack et al., unpublished results).

Acknowledgments

We acknowledge most useful conversations with Professors I. Tinoco, Jr., D. Crothers, and D. H. Turner. We are also grateful to Dr. Jim Howard for sharing with us his unpublished manuscript on the CD of H_2TMpyP-4 with various synthetic polynucleotides at high ionic strength.

Registry No. H_2TMpyP-4, 38673-65-3; H_2TMpyP-2, 59728-89-1; Cu(II)TMpy-4, 48242-70-2; Ni(II)TMpy-4, 48242-71-3; Zn(II)-TMpy-4, 40603-58-5; Co(III)TMpy-4, 51329-41-0; Fe(III)TMpy-4, 60489-13-6; Mn(III)TMpy-4, 70649-54-6; poly(dA-dT), 26966-61-0; poly(dG-dC), 36786-90-0.

References

Bresloff, J. L., & Crothers, D. M. (1981) *Biochemistry 20*, 3547–3553.

Carvlin, M., Dattagupta, N., & Fiel, R. J. (1982) *Biochem. Biophys. Res. Commun. 108*, 66–73.

Dalgleish, D. G., Fujita, H., & Peacocke, A. R. (1969) *Biopolymers 8*, 633–645.

Dalgleish, D. G., Fiel, M. C., & Peacocke, A. R. (1972) *Biopolymers 11*, 2415–2427.

Dattagupta, N., Hogan, M., & Crothers, D. M. (1978) *Proc. Natl. Acad. Sci. U.S.A. 75*, 4286–4290.

Dattagupta, N., Hogan, M., & Crothers, D. M. (1980) *Biochemistry 19*, 5998–6005.

Delays, R. J., & Jackson, D. A. (1976) *Biochem. Biophys. Res. Commun. 69*, 446–454.

Early, T. A., Kearns, D. R., Hillen, W., & Wells, R. D. (1981a) *Biochemistry 20*, 3756–3764.

Early, T. A., Kearns, D. R., Hillen, W., & Wells, R. D. (1981b) *Biochemistry 20*, 3764–3769.

Eaton, S. S., & Eaton, G. R. (1975) *J. Am. Chem. Soc. 97*, 3660–3667.

Eaton, S. S., Fiswild, D. M., & Eaton, G. R. (1978) *Inorg. Chem. 17*, 1542–1545.

Fiel, R. J., & Munson, B. R. (1980) *Nucleic Acids Res. 8*, 2835–2842.

Fiel, R. J., Howard, J. C., Mark, E. H., & Dattagupta, N. (1979) *Nucleic Acids Res. 6*, 3093–3118.

Hambright, P., Gore, T., & Burton, M. (1976) *Inorg. Chem. 15*, 2314–2315.

Harriman, A., & Porter, G. (1979) *J. Chem. Soc., Faraday Trans. 2 75*, 1532–1542.

Hoard, J. L. (1975) in *Porphyrins and Metalloporphyrins* (Smith, K. M., Ed.) pp 317–380, Elsevier, The Netherlands.

McGhee, J. D., & von Hippel, P. H. (1974) *J. Mol. Biol. 86*, 469–489.

Müller, W., & Crothers, D. M. (1968) *J. Mol. Biol. 35*, 251–290.

Müller, W., Crothers, D. M., & Waring, M. J. (1973) *Eur. J. Biochem. 39*, 223–234.

Pasternack, R. F., & Cobb, M. A. (1973) *J. Inorg. Nucl. Chem. 35*, 4327–4339.

Pasternack, R. F., Huber, P. R., Boyd, P., Engasser, G., Francesconi, L., Gibbs, E., Fasella, P., Venturo, C. G., & Hinds, L. C. (1972) *J. Am. Chem. Soc. 94*, 4511–4517.

Pasternack, R. F., Francesconi, L., Raft, D., & Spiro, E. (1973) *Inorg. Chem. 12*, 2606–2611.

Pasternack, R. F., Sprio, E. G., & Teach, M. (1974) *J. Inorg. Nucl. Chem. 36*, 599–606.

Pasternack, R. F., Lee, H., Malek, P., & Spencer, C. (1977) *J. Inorg. Nucl. Chem. 39*, 1865–1870.

Peacocke, A. R., & Sherrett, J. N. H. (1956) *Trans. Faraday Soc. 52*, 261–269.

Scheidt, W. R. (1974) *J. Am. Chem. Soc. 96*, 84–91.

Schmechel, D. E. V., & Crothers, D. M. (1971) *Biopolymers 10*, 465–480.

Sobell, H. M. (1980) in *Nucleic Acid Geometry and Dynamics* (Saima, R. H., Ed.) pp 280–323, Pergamon Press, New York.

Sobell, H. M., Tsai, C.-C., Jain, S. C., & Gilbert, S. G. (1977) *J. Mol. Biol. 114*, 333–365.

Tinoco, I., Jr., & Cantor, C. R. (1970) *Methods Biochem. Anal. 18*, 81–98.

Wells, R. D., Larson, J. E., Grant, R. C., Shortle, B. E., & Cantor, C. R. (1970) *J. Mol. Biol. 54*, 465–497.